Liquid Crystals
Publication details, including instructions for authors and subscription information:
http://www.informaworld.com/smpp/title~content=t713926090

The Ericksen number and Deborah number cascades in sheared polymeric nematics

R. G. Larson[a]; D. W. Mead[ab]
[a] AT&T Bell Laboratories, Murray Hill, New Jersey, U.S.A. [b] Shell Development Co., Houston, Texas, U.S.A.

To cite this Article Larson, R. G. and Mead, D. W.(1993) 'The Ericksen number and Deborah number cascades in sheared polymeric nematics', Liquid Crystals, 15: 2, 151 — 169
To link to this Article: DOI: 10.1080/02678299308031947
URL: http://dx.doi.org/10.1080/02678299308031947

LIQUID CRYSTALS, 1993, VOL. 15, NO. 2, 151–169

The Ericksen number and Deborah number cascades in sheared polymeric nematics

by R. G. LARSON*† and D. W. MEAD†‡

† AT&T Bell Laboratories, Murray Hill, New Jersey 07016, U.S.A.

‡ Shell Development Co., P.O. Box 1380, Houston, Texas 77251, U.S.A.

(*Received 22 December 1992; accepted 18 March 1993*)

Samples of liquid crystalline poly(γ-benzyl-glutamate) solutions are sheared between glass surfaces with gaps, $d = 10$–$500\,\mu$, and shearing velocities, $V = 0{\cdot}05$–$10\,000\,\mu s^{-1}$ so that the Ericksen number $E \equiv Vd\gamma_1/K$ is varied over a large range, $E \approx 1$–10^7. Here γ_1 is the rotational viscosity and K_1 is the Frank splay constant, with γ_1/K_1 estimated to be approximately $1\,s\,\mu^{-2}$ for our samples. We observe by polarizing microscopy a sequence of transitions with increasing Ericksen number analogous to that observed in small molecule tumbling nematics: namely rotation of the director out of the shearing plane and into the vorticity direction at $Vd \approx 25\,\mu^2\,s^{-1}$, and formation of roll cells at $Vd \approx 50\,\mu^2\,s^{-1}$. The roll cells become finer with increased Vd in accord with predictions of linear stability theory using the Leslie–Ericksen equations, and at $Vd \gtrsim 500\,\mu^2\,s^{-1}$, the cells become very irregular, producing director turbulence. The turbulence becomes finer in scale as Vd increases, reaching sub-micron, and possibly molecular scales when $Vd \geqslant 10^5\,\mu^2\,s^{-1}$. At the highest velocities, transitions in orientation and texture are controlled by the Deborah number $De \equiv \lambda V/d$, where λ is the molecular relaxation time, and uniform texture-free samples are obtained when $De \gtrsim 5$.

1. Introduction

When a nematic liquid is sheared steadily between two parallel plates by displacing one plate parallel to itself, the behaviour of the nematic director depends drastically on the sign of α_3/α_2, where α_3 and α_2 are two of the Leslie viscosities [1]. For small molecule nematics at temperatures well away from any transition to a smectic phase, α_3/α_2 is usually positive, and the nematic is flow-aligning [2–4], in the opposite case where $\alpha_3/\alpha_2 < 0$, the director tumbles [5, 6]. At high shear rates, the director in a flow-aligning nematic tends toward a preferred alignment angle at which the viscous torques on the director vanish; this angle is usually a few degrees away from the flow direction. In a tumbling nematic, on the other hand, there is no angle at which viscous torques disappear, and the flow is subject to an extraordinary cascade of instabilities, leading at high shear rates to director turbulence [7–10].

Director turbulence is a chaotic state characterized by an irregular director pattern, and by a profusion of singular lines, or disclinations, at which the director abruptly changes direction. Director turbulence differs from inertial turbulence in ordinary liquids in that the former occurs in fluids of lower i.e. nematic, symmetry, which support topological defects, and in that director turbulence is driven, not suppressed, by viscous forces. Director turbulence occurs in tumbling nematics at a high value of the Ericksen number, here defined as $E \equiv \gamma_1 Vd/K_1$, where γ_1 is the rotational viscosity given in terms

* Author for correspondence.

0267–8292/93 $10·00

of Leslie–Ericksen viscosities by $\gamma_1 \equiv \alpha_3 - \alpha_2$, V the velocity of the moving plate, d the gap between the plates, and K_1 is the Frank splay elastic constant. Despite the differences between them, we shall see that director turbulence, like inertial turbulence, can be accessed via a roll-cell instability akin to that of inertial Taylor–Couette flow [11–14].

Study of director turbulence might well be essential to gain an understanding of shearing flows of most polymeric nematics, for which it now appears, tumbling is the norm [15–20]. The increasing use of lyotropic and thermotropic polymeric nematics as specialty high strength or high modulus materials is fuelling increased interest in the processing, and hence the flow properties, of these fluids. Since the viscosities of polymeric nematics are invariably high, $\gamma_1 \gtrsim 10^2$ poise, the Ericksen number in flows of these fluids is also almost always high, i.e. $E \sim 10^4$–10^6 or higher, and the flow can be highly turbulent.

Because of their lower viscosities, which are typically around 0·1–1·0 poise, Ericksen numbers are usually smaller than this in shearing flows of small molecule nematics. For small molecule tumbling nematics, the first stages of the cascade to turbulence have been studied in some detail, both experimentally and theoretically [6, 7, 21–32]. If the director is initially uniformly aligned homeotropically, that is, normal to the shearing surfaces, and is strongly anchored to the surfaces in that alignment, then weak shearing, i.e. with $E \leqslant 1$, produces in the bulk a slight tipping of the director toward the flow direction, with the maximum tip occurring at the midplane between the two shearing surfaces (see figure 1 (*a*)). As E increases, the angle of tip at the midplane, θ_0, also increases, and, since there is no angle at which viscous torques on the director vanish, the increase in tipping does not saturate when E becomes large [27]. Instead, θ_0 continues to increase, eventually reaching, and exceeding, 90°, which is the flow direction (see figure 1 (*b*)). With further increases in E, so that $E = 10$–100, or higher, depending strongly on the values of the nematic viscosities and elastic constants [29], θ_0 can undergo one or more 'tumbling transitions' in which θ_0 increases discontinuously [8, 27]. At some point roughly in this same range of Ericksen numbers, the flow becomes unstable to a secondary flow that takes the director out of the shearing plane [23, 29–33] (see figure 1 (*c*)). The shearing plane is defined as to be parallel to both the flow and the homeotropic directions. Still further increases in E tip the director further and further out of the shearing plane [31–33], until it is nearly orthogonal to that plane [6], and hence is nearly parallel to the vorticity direction (see figure 1 (*d*)). Then, when E becomes even higher still, around 1000 for the tumbling nematic HBAB [6, 34], the flow becomes unstable to the formation of roll cells oriented parallel to the flow direction [6]. These roll cells are produced by a secondary flow that is periodic in the vorticity direction [21–25].

The formation of rolls can be studied most simply if the anchoring condition and the initial orientation of the director are both parallel to the vorticity direction (see figure 2). For a sample that is initially homogeneously oriented in the vorticity direction, the tumbling and out-of-plane transitions discussed above do not occur, and shear does not affect the director orientation at low E. However, when E reaches 100–1 000, the roll cells, shown in figure 2, are formed [35]. Linear stability analyses predict the structure and onset condition for the rolls [22, 35]. At values of E well above the onset condition, disclination lines are somehow generated in abundance, and the flow takes on the characteristics of director turbulence [8–10]. Here, we shall probe the transitions to roll cells and to director turbulence in polymeric nematics. Polymeric nematics are well suited to studying these transitions, because the required range of

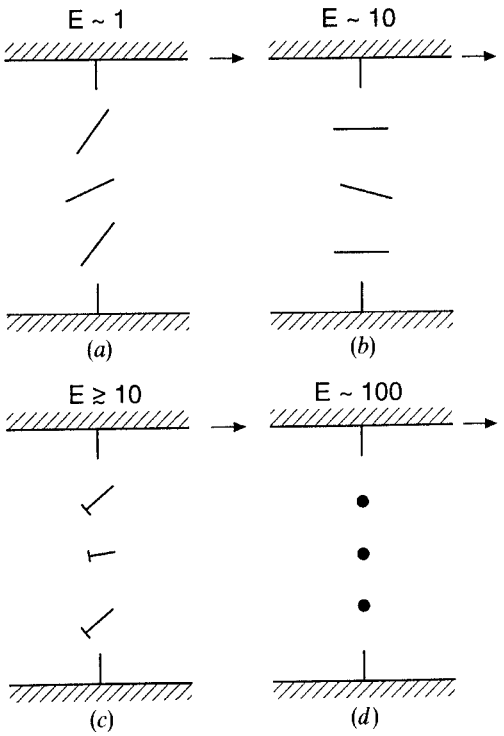

Figure 1. Sequence of transitions in the director profile of a tumbling nematic as it is sheared with ever increasing Ericksen number. The Ericksen numbers cited at each stage are illustrative; actual values of E vary considerably depending on material constants. See text for details.

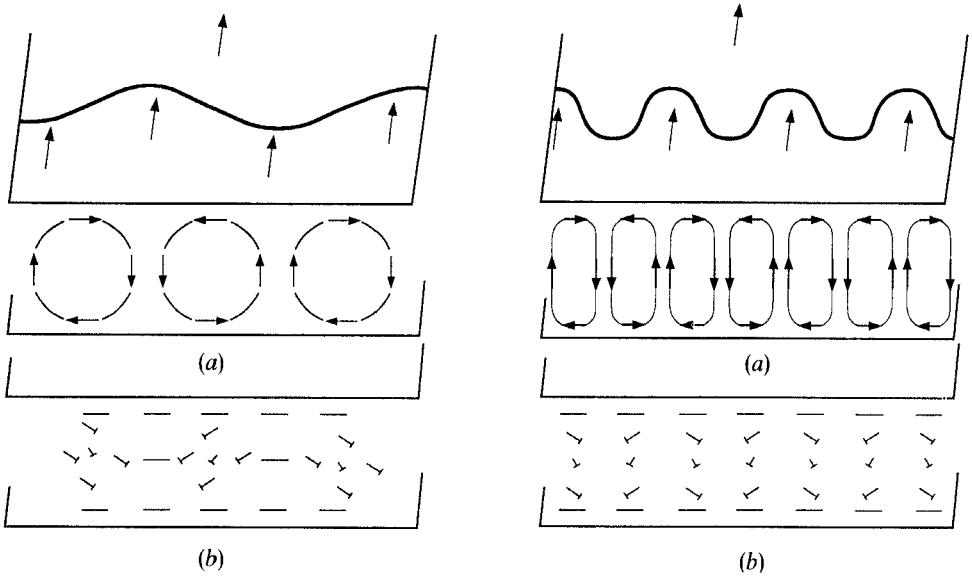

Figure 2. Velocity field (*a*) and director field (*b*) of the most unstable roll cells predicted for plane Couette flow with the director initially in the vorticity direction. Just above the critical Ericksen number, the most unstable rolls are predicted to be roughly square as on the left, while well above the critical Ericksen number the most unstable rolls are thin, as on the right.

Ericksen numbers ($E \approx 1$–10^4) is attained at such low velocities that the time evolution of the director field can be followed easily. In fact, for polymeric nematics, roll cells form at such low shear rates that one must reduce the shear rate to an extraordinarily low value to avoid them. Roll cells in the polymeric nematic PBT (poly(1,4-phenylene-2,6-benzobisthiazole)), were observed by Srinivasarao and Berry [17] even at the lowest shear rates they examined.

At high shear rates, the viscous torques in polymeric nematics can even become large enough to influence the dynamics of individual molecules. Thus the molecular order parameter of some polymeric nematics can be distorted at shear rates of only $10\,s^{-1}$ or so [18–20]; such distortions of the order parameter never occur in small molecule nematics at reasonably accessible shear rates. As we shall see, these order parameter distortions produce a series of high shear rate transitions in the texture and flow properties that are controlled not by the Ericksen number, but by the Deborah number, $De \equiv \lambda V/d$, where λ is the molecular relaxation time of the polymeric nematic.

2. Experimental

The shearing cell used here consists of two optically flat borosilicate glass windows, $1'' \times 3''$, that are made nearly parallel by observing Fizeau fringes. The fringes show that the plates are flat to within a couple of microns. The gap between the plates can be controlled between $10\,\mu$ and a few centimetres with a precision of $5\,\mu$. The upper plate translates almost perfectly parallel to itself at speeds ranging from $0{\cdot}05$–$10^4\,\mu\,s^{-1}$, driven by a wormscrew and motor. A 100 : 1 speed-reducing gear is used to attain the lowest speed of $0{\cdot}05\,\mu\,s^{-1}$. Thus, with a $100\,\mu$ gap, the shear rate $\dot{\gamma}$ can be made as low as $5 \times 10^{-4}\,s^{-1}$, or as high as $10^2\,s^{-1}$. The shearing cell is mounted in place of the stage of a polarizing microscope to permit observation of the director field; for more details, see elsewhere [36].

The fluids studied here include racemic, and hence nematic, mixtures of PBLG, poly(γ-benzyl-L-glutamate), with its enantiomorph PBDG, dissolved in the solvent metacresol (*m*-cresol). Two racemic solutions are studied, namely PBG198, a 15 per cent by weight solution with polymer molecular weight 198 000, and PBG118, a 22 per cent solution with molecular weight 118 000. Values of γ_1/K_1 for the PBG solutions of similar concentration and molecular weight were reported by Lee and Meye [37] (solution Nos 8 and 11 in [37]). From these, we estimate that $\gamma_1/K_1 \approx 1{\cdot}0\,s\,\mu^{-2}$ for PBG118 and $\approx 1{\cdot}4\,s\,\mu^{-2}$ for PBG198. Thus for PBG118, values of the product Vd, if reported in units of $\mu^2\,s^{-1}$, are numerically equal to the Ericksen number, while for PBG198, $E \approx 1{\cdot}4Vd$ in these units. With these two fluids, and the range of gaps and velocities available, the Ericksen number in our shear cell can easily be varied over a wide range, 1–10^7.

At high shear rates, results are also reported for cholesteric PBLG238 and PBDG298. PBLG238 is a 13·5 per cent solution of a polymer of molecular weight 238 000 which we reported on earlier [38], although in the earlier study the concentration was 12·5 per cent. The 13·5 per cent solution, however, is one of those whose birefringence was measured by Hongladarom *et al.* [39], and we shall later compare some of our microscopic observations with these birefringence measurements. PBDG298 is a 13 per cent solution of molecular weight 298 000 and was chosen because its average molecular relaxation time, λ (defined later), is about 0·10 s, higher than that of the other solutions. For PBLG238 and PBDG298, our studies are limited to shear rates high enough to destroy any cholesteric textures, and render the fluid effectively nematic.

Except for PBDG298, the PBG solutions studied here at room temperature, around 22°C, have relaxation times, λ, that are less than about 0·05 s. When the Deborah number, $De \equiv \lambda V/d$ is less than 0·1 or so, we expect that the Leslie–Ericksen theory should provide a valid description of the flow behaviour of these fields. This implies that for a gap of 100 μ, the Leslie–Ericksen theory should be applicable as long as $V \lesssim 200\,\mu\,s^{-1}$, or $Vd \lesssim 2 \times 10^4\,\mu\,s^{-1}$.

For nematic PBG solutions, the nematic director anchors itself homeotropically at the glass surfaces. When these clean surfaces are brought to within about 10–15 μ of each other, both PBG118 and PBG198 spontaneously orient homeotropically throughout the thin gap, creating areas as large as 4 mm^2 that are uniform and disclination free [36]. For larger gaps, $d \geqslant 25\,\mu$, the quiescent fluid does not free itself of disclinations within acceptable time periods. However, for gaps of 25–100 μ, a roughly uniform starting state can be prepared over regions as large as 1 mm^2 by shearing PBG198 at velocities of around 0·2–1·0 s^{-1}, as discussed in the following.

3. Results

3.1. *Low shear rates*

In earlier work [36, 38], we showed that shearing 10–400 μ thick samples of PBG198 at shear rates of 0·04 s^{-1} or higher produces a striped birefringence texture under crossed polarizers with stripes parallel to flow, and steady-state stripe spacings of 10 μ or less. Defect lines that are generally parallel to flow accompany these birefringent stripes, and have a similar spacing. Polarimetry studies using a quarter-wave plate showed that the birefringent stripes are a manifestation of variations in director orientation that are periodic in the vorticity direction.

Despite the low shear rates of these previous studies, the Ericksen numbers were still high, namely $E \geqslant 500$ for $d = 100\,\mu$ and $E \geqslant 50$ for $d = 10\,\mu$, and stripes formed for PBG198. Here, using velocities as low as 0·05 $\mu\,s^{-1}$, the Ericksen number is brought below unity for $h \approx 10\,\mu$, and as low as $E \approx 5$ for $d \approx 100\,\mu$. At these low Ericksen numbers, the stripes are avoided altogether, as discussed below. The low velocities used in these cases permitted photographs to be taken during shear flow, with negligible fluid motion during exposure, with exposure times which were around 1 s.

For PBG118 with $d \approx 10\,\mu$, homeotropic monodomains form under quiescent conditions, as shown by observing that the sample is black under both crossed 0°–90° and 45°–135° polarizers. Here 0° is the direction of flow and 90° is the vorticity direction. When these monodomains are sheared at $V < 5\,\mu\,s^{-1}$ ($E < 50$), the director rotates toward the flow direction, but remains within the plane of shear. For higher values of V, the director leaves the plane of shear and a chaotic texture is produced. For PBG198 with $d \approx 10\,\mu$, homeotropic monodomains also form. For these, when $V \geqslant 5\,\mu\,s^{-1}$, the director also exits the shearing plane, but does so by producing a periodic 'band' pattern, with bands oriented in the vorticity direction, as shown elsewhere [36]. These bands do not form during shearing of PBG118, possibly because the ratios of Leslie viscosities diverge from unity to a lesser extent for PBG118 than they do for PBG198. In magnetically induced reorientations of the director field in PBG solutions, band patterns orthogonal to the applied field also form; they form because of a periodic secondary flow that permits more rapid reorientation of the director than would be possible if the director were to rotate without such a secondary flow [40]. The rate of director rotation in the absence of secondary flow is controlled by the rotational viscosity γ_1, which is much larger than the viscosities controlling the secondary flow, the more so as the molecular weight of PBG increases [37]. If a large value of γ_1 is also

responsible for formation of bands during shearing of PBG198, then the lack of such bands in PBG118 might be explained by the factor of two or so smaller value of γ_1 expected for PBG118, as compared to PBG198.

For thicker gaps, $d \geqslant 25\,\mu$, homeotropic monodomains do not form within the time scale of our experiments, which is at most a few days. However, for PBG198, a relatively uniform director field can still be produced in samples with gaps of 25–100 μ, if they are sheared for several hours at rates such that $5 \leqslant Vd \leqslant 25$. Under these conditions, the texture of PBG198 becomes very coarse and the alignment is preferentially in the vorticity direction. Figure 3 shows a 50 μ thick sample under a steady-state shear at $V = 0{\cdot}5\,\mu\,s^{-1}$ ($Vd = 25$) under crossed 45°–135° polaroids with and without a quarter-wave plate inserted between the sample and the analyser, with the slow axis of the quarter-wave plate parallel to the vorticity direction. Insertion of the quarter-wave plate changes the colour of the sample from blue–white to yellow–orange, a shift up Newton's colour scale, which shows that the average orientation is parallel to the slow axis of the quarter-wave plate, and hence parallel to the vorticity direction [36]. When the slow axis of the quarter-wave plate is parallel to the flow direction, the sample darkens, as expected, since the director is perpendicular to the flow direction. As discussed in the Introduction, according to both theory and experiments for tumbling small molecule nematics, shearing flow with $E \sim 100$ orients the director predominantly in the vorticity direction. Figure 3 shows that the same phenomenon occurs in a polymeric nematic, PBG198.

Notice in figure 3 the faint ripples that are aligned more or less parallel to flow. These ripples at $Vd = 25\,\mu\,s^{-1}$ are the precursors to the well-defined stripes that form when Vd is increased to $50\,\mu^2\,s^{-1}$ or greater. Figure 4 shows the formation of these stripes for $d = 100\,\mu$ and $V = 1{\cdot}5\,\mu\,s^{-1}$; i.e. $Vd = 150\,\mu^2\,s^{-1}$, respectively 9 min and 12 min after start-up of shearing, which correspond to 8 and 11 strain units, respectively. In figure 4 the stripes are viewed between crossed 0°–90° polarizers with a quarter-wave plate inserted at 45°. After 20 min of shearing under these conditions, the stripes become sharply defined, as shown under higher magnification in figure 5. Note in figure 5 that disclination lines have formed between the dark and light stripes. The birefringence patterns in figures 4 and 5 show that during shear, the director tips away from its initial orientation (which was in the vorticity direction), and that the degree of tip is roughly periodic in the vorticity direction.

Figure 6(*b*) shows an analogous periodic variation in the light intensity when the analyser is absent after 9 min of shear. The periodic pattern of light intensity in figure 6(*b*) is called a 'phase grating', and it shows that there is a periodic tipping of the director out of the plane of the sample, which, because it creates a periodic variation in refractive index, focuses the light in some regions of the sample and defocuses it in others, thus producing variations in light intensity when only one polarizer is present. The presence of both the phase grating and the birefringent stripe pattern shows that shear flow causes the director to tip away from the vorticity direction both within the sample plane and out of the sample plane. This pattern of director tipping, and the direction in which the pattern is periodic (the vorticity direction), are consistent with the formation of roll cells (see figure 2). As mentioned in the Introduction, roll cells have also been both predicted and observed in small molecule nematics, and in the polymeric nematic PBT.

The phase grating in figure 6(*b*) is imaged by focusing either above or below the plane of the sample by a few hundred microns. The pattern of dark and light obtained by focusing above the sample is almost identical to that obtained when one focuses

below the sample, except that the light and dark areas are inverted. This symmetry in the phase grating implies that the degree of downward tip in some regions of the sample is comparable to the degree of upward tip in other regions. After 20 min of shearing, this symmetry is broken; when one focuses above the plane of the sample dark lines are observed (see figure 6(*c*)), and below the plane of the sample these dark lines are replaced by slender light areas separated by thin parallel lines (see figure 6(*c'*)). We identify these lines as order 1 disclinations, since they are thick compared to the order 1/2 disclinations that can be observed, along with order 1 lines, in highly textured quiescent samples. Thus, figure 6 shows shear-induced nucleation of disclination lines in an originally disclination-free region of the sample.

The relationship of these disclinations to the striped birefringence texture is shown in figure 5. Figure 5 shows that the disclination lines are located between the yellow and black birefringent regions. Thus, projected into the sample plane, the direction of director tip with respect to the vorticity direction changes sign as one passes through the disclination line. This seems to imply that the disclination lines usually reside between the roll cells and thus, not surprisingly, in the regions where the tip out of the plane of the sample is maximum. One might well imagine that these disclination lines are produced when the degree of tip out of the sample plane becomes large enough to lead to a localized tumbling transition similar to the global tumbling transitions that can occur at lower Ericksen numbers when the director resides within the shearing plane [27].

At lower Ericksen numbers in the range $50 \leqslant Vd \leqslant 100$, the stripes still appear, but are weaker; the phase grating is also weaker, and disclination lines are not nucleated. The steady-state birefringence and phase grating at $Vd = 50$ are similar to the transient early-time pattern for $Vd = 150$ shown in figure 4. These weak roll cells disappear, not only when flow ceases, but also when the velocity is reduced below the critical value for roll cell formation. Hysteresis is small, or non-existent. Thus the bifurcation to roll cells appears to be a supercritical one, and arbitrarily weak roll cells can be stabilized at values Vd only slightly above critical. Observation of the birefringence patterns in these weak roll cells when the crossed polarizers are rotated shows that the departure of the director from orientation in the vorticity direction toward the flow direction is small when the roll cells first appear, but increases continuously as Vd is increased, reaching about 20° at $Vd \approx 75$, 45° at $Vd \approx 150$, and significantly exceeding 45° when $Vd \approx 500$.

The disclination lines are not straight, but wavy, perhaps because the initial director field is not completely uniform. The lines are of finite length, fading in intensity and disappearing as one follows them in space. (By refocusing the sample, we verified that the lines really disappear, and have not simply passed out of focal position.) Also, remarkably, for $150 \leqslant Vd \leqslant 500$, each disclination line, like a soliton, translates in the shearing field without changing its intensity or irregular shape. Instead, each kink or

---

Figure 3. PBG198 at a gap of 50 μ and a velocity V of 0·5 $\mu\,s^{-1}$ after 140 min of shearing under two polarization conditions. In these and the following figures, the flow direction is always horizontal, and, except where noted, the sample is viewed through a × 5 objective and the width of the field of view is 2 mm across. $Vd = 25\,\mu\,s^{-1}$.

Figure 4. PBG198 at a gap of 100 μ and a velocity V of 1·5 $\mu\,s^{-1}$ after (*a*) 0 min; (*b*) 9 min, and (*c*) 11 min of shearing between crossed 0°–90° polarizers with a quarterwave plate inserted with slow axis at 45°; $Vd = 150$.

Figure 5. As figure 4, except about 20 min have elapsed and the sample is viewed with a × 20 objective, with a field of view of 0·49 mm across.

Figure 3.

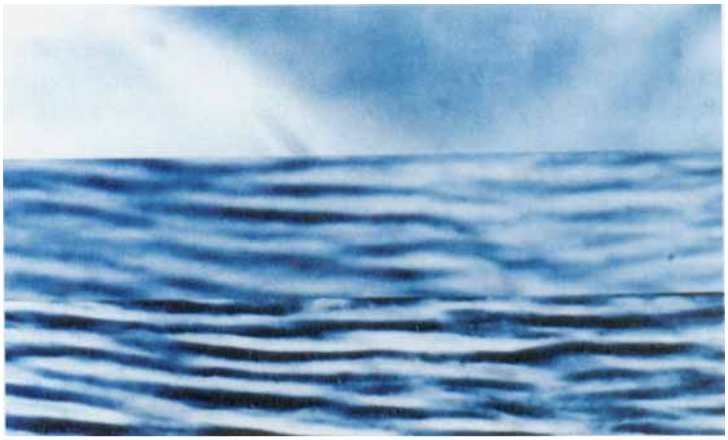

Figure 4.

Figure 5.

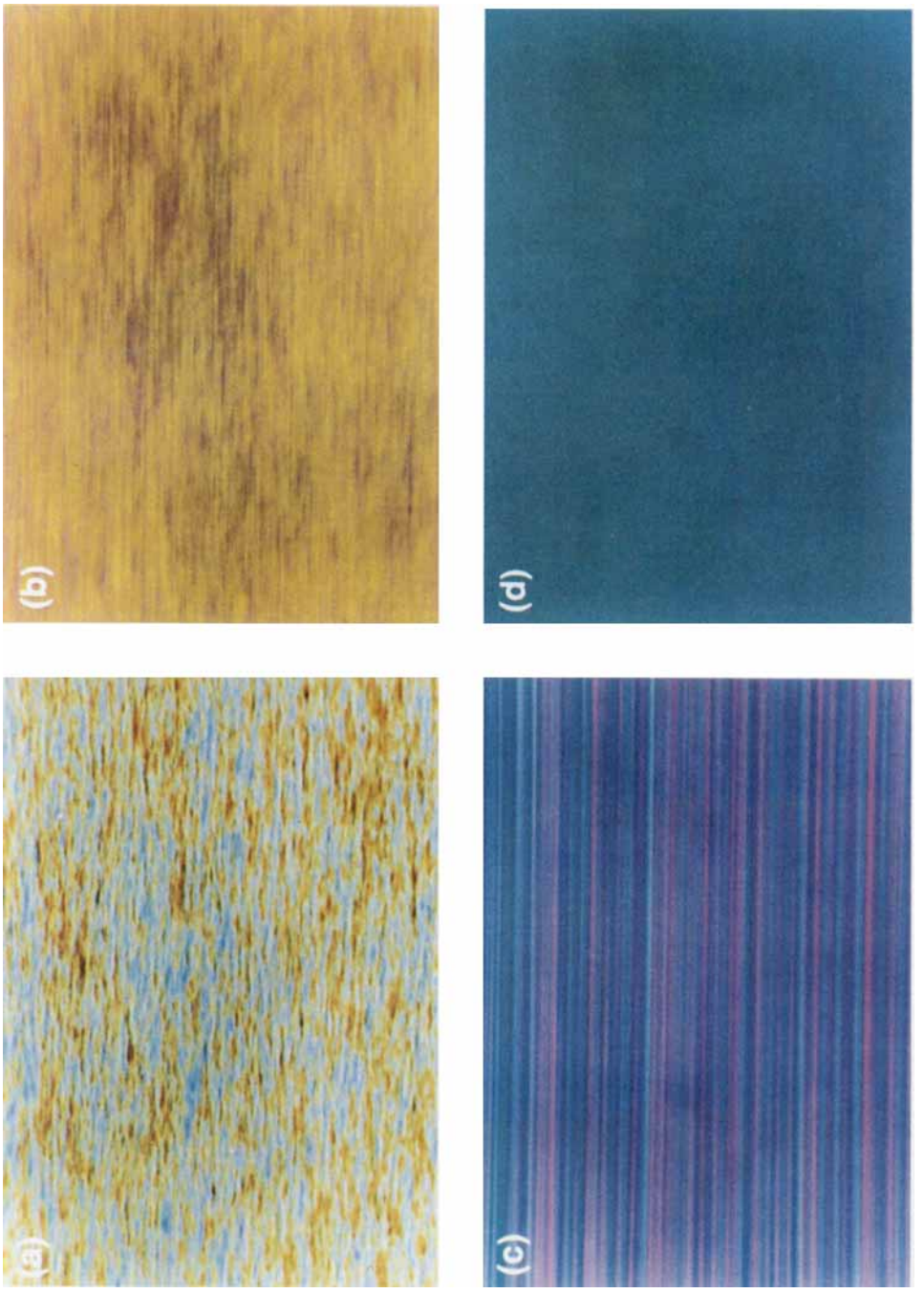

Figure 9. Texture between crossed 45°–135° polarizers, produced by shearing PBLG238 at a gap of 250 μ and shear rates $\dot{\gamma}$ of (*a*) 0·1, (*b*) 1, (*c*) 10 and (*d*) 40 s^{-1} for at least 100 strain units. Here the sample is viewed through a $\times 10$ objective, with a field of view 0·97 mm across. Although there are no stripes in (*d*) at 40 s^{-1}, stripes are visible at this shear rate if the polaroids are rotated to 10°–100°. However, no stripes can be seen under any polarization conditions when $\dot{\gamma} > 75\,s^{-1}$.

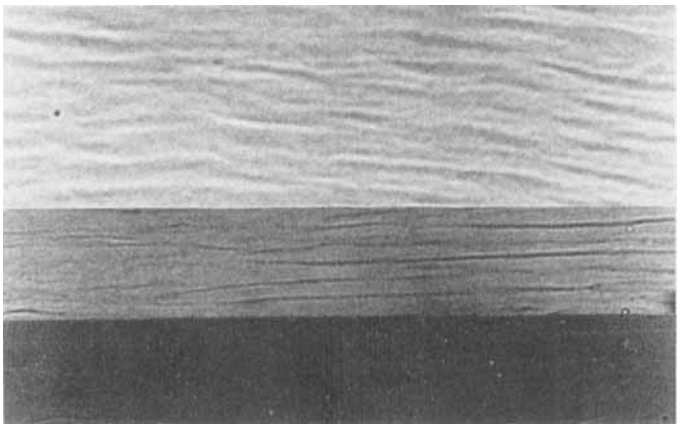

Figure 6. As figure 4, except that the sample is viewed without the analyser and without the quarterwave plate. In (*b*), the sample is viewed after 11 min of shearing and in (*c*) and (c′), 20 min have elapsed. In (c), the focal position is a couple hundred microns above the sample, while in (c′), the focus is below the sample.

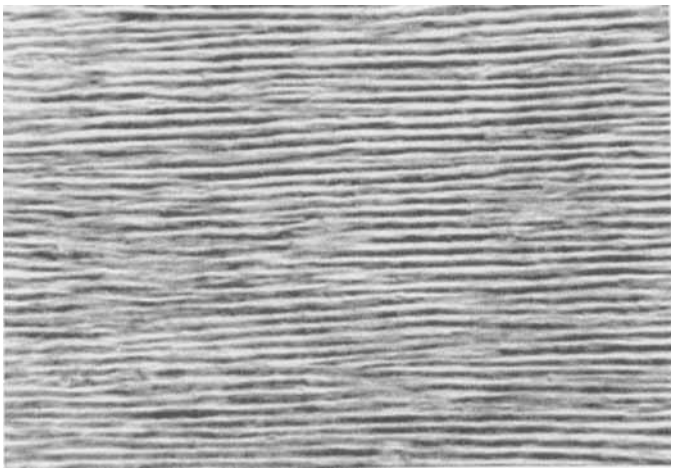

Figure 7. Thin stripes for PBG198 at a gap of 25 μ and a velocity of 3·5 $\mu\,s^{-1}$ after 9 min of shearing. The sample is viewed between crossed 0°–90° polarizers, with a quarter-wave plate inserted with slow axis at 45°. $Vd = 87{\cdot}5\,\mu^2\,s^{-1}$.

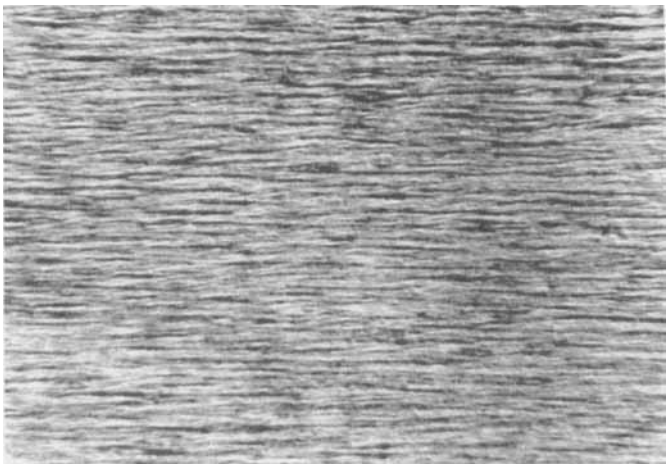

Figure 8. Irregular stripes observed for PBG198 at a gap of 50 μ and a velocity of 10 $\mu\,s^{-1}$ after 3 min of shearing, viewed under the same polarization conditions as figure 7. $Vd = 500\,\mu^2\,s^{-1}$.

wave in each line stays the same while that line translates millimetres across the field of view of the microscope. However, for $Vd > 500$, the intensity and shape of the lines fluctuate during flow. For each gap, d, as V is increased, the spacing, b, decreases between the dark birefringent stripes that appear under crossed 0°–90° polarizers with a 45° quarter-wave plate; b also decreases with decreasing gap, d, for fixed V. For example, figure 7 shows a 25 μ thick sample of PBG198 after it had been sheared for 9 min at $V = 3{\cdot}5\,s^{-1}$. Note how much thinner the stripes are under these conditions than they are for smaller V and larger d in figure 4.

Figure 8 shows that at still higher V, namely $V = 10\,\mu\,s^{-1}$ at $d = 50\,\mu$, a fine structure quickly develops (within 3 min) that is superimposed on what appears to be a dominant stripe spacing. Even at lower Vd, $Vd \approx 150$–500, if shearing is prolonged for 50 or more strain units, a weaker fine structure appears, which disrupts somewhat the regularity of the striped pattern. As V increases, the fine structure becomes even more intense, and the pattern becomes less and less coherent.

3.2. *High shear rates*

For $E \sim 10^3$–10^6, the texture becomes finer and finer, until it is below optical microscopic resolution, and finally, we believe, reaches the molecular length scale, which for our PBG molecules is around 0·1 μ. We examined PBLG238 and PBDG298 at gaps $d = 25$–$500\,\mu$ and at shear rates $\dot{\gamma} = 0{\cdot}1$–$200\,^{-1}$. These two fluids were studied because they have relatively long molecular relaxation times, 0·05 s, and 0·10 s, respectively, and the birefringence of one of them, PBLG238, was measured earlier by Hongladarom *et al.* [39]. Both of these fluids show a similar sequence of changes in texture and colour as $\dot{\gamma}$ increases, shown for PBLG238 in figure 9. First, there is a mottled or 'speckled' texture with texture length scales that become finer as the shear rate increases (see figures 9 (*a*) and (*b*)). This gives way at increased $\dot{\gamma}$ to a recurrence of distinct stripes parallel to flow, which at these high shear rates are unbroken and very straight (see figure 9 (*c*)). These become more intense and then less intense as $\dot{\gamma}$ increases, and finally disappear entirely at still higher $\dot{\gamma}$, and the sample then becomes uniform in colour, with no evidence of texture (see figure 9 (*d*)). Similar stripes and a texture-free 'monodomain' were induced at high shear rates in recent experiments of Mather [41]. This shear-induced monodomain can remain free of texture for many hours after flow has ceased. For this sample at lower shear rates, $0{\cdot}2 \lesssim \dot{\gamma} \lesssim 30\,s^{-1}$, after cessation of shearing, birefringent bands form that are orthogonal to the previous flow direction [36]; but for $\dot{\gamma} = 100\,s^{-1}$, these bands usually do not form.

As the above texture changes are occurring with increasing $\dot{\gamma}$, there is a simultaneous change in the sample's average colour under crossed 45°–135° polarizers (see figures 9 (*a*)–(*d*)). This change in colour corresponds to an increase in the average birefringence with increased shear rate, according to Newton's colour scale. Insertion of a quarterwave plate shows that the alignment for each of these shear rates is preferentially in the flow direction. The gap in figures 9 (*a*)–(*d*) is 250 μ and the shear rates are 0·1, 1, 10 and $40\,s^{-1}$, each after more than 100 units of shearing. At $\dot{\gamma} = 0{\cdot}1\,s^{-1}$, the colour (in figure 9 (*a*)) is mainly orange, with streaks or 'speckles' of blue; on Newton's colour scale the orange corresponds to a retardance around 450 nm. At $\dot{\gamma} = 10\,s^{-1}$, the texture in (figure 9 (*b*)) is extremely fine, with a characteristic length scale of not much more than a micron; the colour, predominantly orange-red, corresponds to a retardance around 500 nm, and the range of colours is far less than in figure 9 (*a*). At $\dot{\gamma} = 10\,s^{-1}$ there is (in figure 9 (*c*)) a recurrence of distinct stripes with width around 10 μ; and the predominant colour is purple, corresponding to a retardance of 550 nm.

Finally, at $\dot{\gamma}=40\,s^{-1}$, the texture is a uniform blue–green, corresponding to a retardance of 800 nm, and there is no remaining sign of texture.

Examination of this sample under other polarization conditions, in the shear rate range $\dot{\gamma}=0{\cdot}1$–$200\,s^{-1}$ and with gaps of 25–500 μ shows that the distinct stripes shown in figure 9 (*c*) exist in the shear rate range 7–75 s^{-1}. These stripes are most readily visible under crossed 10°–100° polarizers, and are sometimes not seen under crossed 45°–135° polarizers even when visible under crossed 10°–100° polarizers. In figure 9 (*d*), for example, stripes are not seen at $\dot{\gamma}=40\,s^{-1}$, but they are visible if the polarizers are rotated to 10°–100°. At a higher shear rate, $\dot{\gamma}=80\,s^{-1}$, no stripes are visible under any polarization conditions. The shear rates at which the texture changes from speckled to distinct stripes to uniform monodomain are independent of the gap, which indicates that these changes in texture are controlled by the Deborah number $De\equiv\lambda\dot{\gamma}$, not the Ericksen number E. This conclusion is confirmed by our observations with PBDG298, which shows the same progression in textures as PBLG238 but the shear rates at which the changes occur for PBDG298 are half as large as they are for PBLG238. As discussed later, λ for PBDG298 is twice as large as for PBLG238, hence these changes in texture occur at about the same values of the Deborah number for the two samples.

4. Discussion

4.1. *The Ericksen number cascade*

Manneville and Dubois-Violette [22] performed a linear stability analysis for a nematic fluid undergoing steady shearing with director initially oriented uniformly in the vorticity direction. This analysis used the Leslie–Ericksen equations to describe the dynamics of the nematic, and predicted that both tumbling and non-tumbling nematics are unstable to the formation of roll cells that are parallel to flow at a critical value of the Ericksen number E_{roll}. Since non-tumbling nematics in this initial orientation are unstable also to a homogeneous instability that at $E_{homog}<E_{roll}$ rotates the director toward the flow aligning angle, the rolls should not, and indeed are not, seen in non-tumbling nematics, unless a magnetic field is used to block the homogeneous instability. For tumbling nematics, there is no homogeneous instability, and roll cells form when $E\geqslant E_{roll}$.

Recently, one of us (R.G.L.) extended the analysis of Manneville and Dubois-Violette by including the effects of finite rates of roll cell growth [35] for $E>E_{roll}$. It was found that as E increases above E_{roll}, an ever-widening band of roll cell widths becomes unstable, and the fastest growing rolls in this band are predicted to become thinner as E increases.

Figure 10 (*a*) shows that for PBG198 sheared in gaps of 100 μ and 25 μ, the spacing, b, between dark stripes (such as those in figures 4 and 7) does decrease with increased V and decreased d, as predicted. The spacing, b, was obtained by counting the number of well defined stripes that crossed a line of known length running perpendicular to flow, at shearing strains for which the stripes were well defined, usually around 20–40 strain units. (At strains below this range, the stripes had not yet formed or were weak, while at larger strains the stripes became somewhat disrupted by a superimposed fine structure.)

In figure 10 (*b*), the measured relationship between reduced Ericksen number $(Vd)/(Vd)_{roll}$ and the dimensionless stripe width $b/2d$ of the observed roll cell pattern is compared to the predicted relationship between E/E_{roll} and $\pi/2q_{xm}$, where q_{xm} is the wavenumber from the linear theory of the fastest growing roll cells, made dimensionless using the half-gap thickness [35]. Since $b/2$ is the width of a single roll cell, i.e., a single dark or light stripe, $b/2d$ is the measured aspect ratio of the roll cells, and $\pi/2q_{xm}$ is the

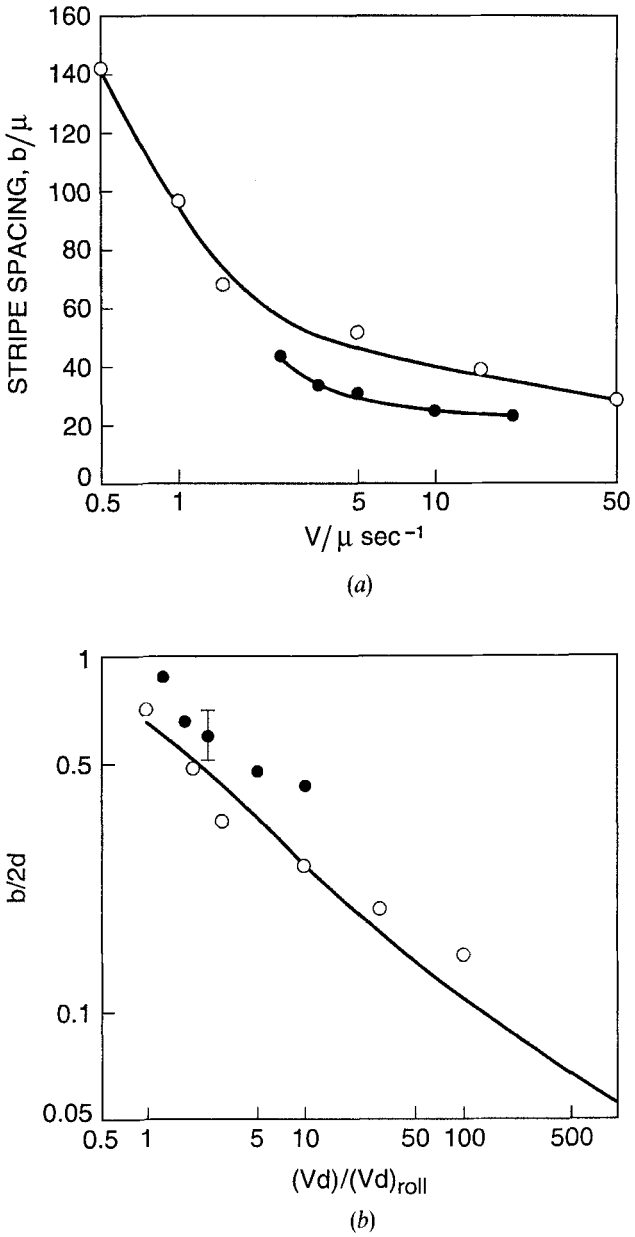

Figure 10. (*a*) Stripe spacing as a function of plate velocity, V, for two different gaps, d, for PBG198. These spacings were measured after strains of 20–40 units were imposed so that the stripes were well defined but had not yet become severely distorted by fine structures. In (*b*), the stripe spacings are plotted in dimensionless form against normalized Vd. Because of the 5 μ uncertainty in the gap, the data for the 25 μ gap are subject to more relative uncertainty than those for $d = 100\,\mu$, indicated by the error bar. The prediction of the linear theory derived in [35] is also shown, (●) $d = 25\,\mu$; (○) $d = 100\,\mu$; (——) = linear theory.

corresponding predicted aspect ratio of the fastest growing rolls. The ratios of Leslie–Ericksen viscosities used in the predictions of the linear theory were taken from the Doi theory for nematic solutions of long monodisperse rigid rod molecules [15] and the ratios of elastic constants were taken to be $K_1/K_3 = 1$, $K_1/K_2 = 10$. While these ratios of elastic constants are consistent with the measurements of Lee and Meyer [37], some of the ratios of viscosities we have taken from the Doi theory may be inaccurate for our solutions, since PBG molecules are far from being ideal monodisperse rigid rods. Also, the linear stability theory was developed for an initially uniform director field oriented in the vorticity direction, while in the experiments the orientation is not completely uniform, and at the glass surfaces director prefers a homeotropic orientation, with an unknown anchoring strength. In addition, since the theory is linear, it can only be expected to be accurate when the roll cells are weak, whereas the experimental roll cell widths were obtained after the cells had become well defined.

Despite these limitations, the theoretical prediction of $\pi/2q_{xm}$ versus E/E_{roll} taken from [35] is in good agreement with the measurements. However, the critical Ericksen number predicted using viscosities from the Doi theory is quite large, $E = (|\alpha_2|\alpha_4)^{1/2} Vd/K_1 = 500$, compared to the observed critical condition $\gamma_1 Vd/K_1 \approx 40$, assuming a value of $\gamma_1/K_1 = 1{\cdot}4\,\mathrm{s}\,\mu^{-2}$ from Lee and Meyer for a similar solution. Since $\gamma_1 \approx |\alpha_2| > \alpha_4$, the discrepancy between the experimental and the theoretical critical conditions is greater than an order of magnitude. However, variations in the Leslie–Ericksen parameters can easily change E_{roll} by an order of magnitude or more [35] and we suspect that some of the discrepancy may come from a divergence of the viscosity ratios of PBG from those predicted by the Doi theory.

Despite this disagreement in E_{roll}, both theory and experiment show a gradual decrease in roll cell width with increased Ericksen number, and the predicted aspect ratios of the roll cells agree with experimental values. Within the range of E over which distinct roll cell spacings could be observed, namely $E_{roll} \approx 70 \leqslant Vd \leqslant 7\,000$, the decrease in roll spacing with increased E lies between the power laws $b \propto E^{-1/4}$ and $b \propto E^{-1/2}$. The finite-growth-rate stability theory shows that for large enough E, the scaling law $b \propto E^{-1/4}$ is approached [35]. However, for E beyond the range covered in figure 10, i.e. $E \geqslant 10^4$, the observed stripe pattern is too irregular for a single dominant stripe width to be obtained by inspection. This is not surprising, since the linear theory predicts that the band of unstable roll cell widths gets wide as E increases, and thus many stripe widths are expected to coexist in the flow. A Fourier analysis [38] of the spectrum of stripe widths at high E ($E \approx 10^5$–10^6) showed a wide spectrum of widths, the average of which decreased with increased $\dot{\gamma}$, roughly consistent with the scaling $b \propto \dot{\gamma}^{-1/4} \propto E^{-1/4}$.

At these high Ericksen numbers, $E \sim 10^4$–10^6, the director field is spatially irregular and time dependent, although it still seems to possess the remnants of a striped pattern, until, as discussed below, the Deborah number, De, becomes large. The changes in the structure of the flow with increased E are similar in some respects to the changes in the structure of Taylor-vortex flow between concentric cylinders as the Reynolds number, Re, increases [13, 14]. At these high-Ericksen-number conditions, $E \sim 10^4$–10^6, spatial variations of the director occur over length scales much smaller than the sample thickness, and the 'domains' of spatial coherence of the director are so small and so numerous that they can perhaps be treated in a statistical manner. One can imagine that by averaging over the large number of such domains that exist in a sample at high Ericksen number, the macroscopic stress and birefringence could be calculated. Some recent theories that take this approach give promisingly good agreement with measured macroscopic stresses [19, 42].

Table 1. Ericksen and Deborah number cascades for $\gamma_1/K_1 \sim 1\,\mathrm{s}\,\mu^{-2}$; $d \sim 100\,\mu$; $\lambda \sim 0{\cdot}05\,\mathrm{s}$.

E or De number	Flow regime	Shear rate, $\dot{\gamma}/\mathrm{s}^{-1}$
$E \sim 1$	In-plane tipping	10^{-4}
$E \sim 10$	In-plane tumbling transition	10^{-3}
$E \sim 10$	Out-of-plane motion	10^{-3}
$E \sim 10^2$	Roll cell formation	10^{-2}
$E \sim 10^3$	Roll cell refinement	10^{-1}
$E > 10^4$	Director turbulence	$\gtrsim 10^0$
$2 \gtrsim 10^3$; $De \lesssim 1$	Domain theories might apply	$10^{-1} \approx \dot{\gamma} \approx 20$
$De \lesssim 1$	Tumbling	$\lesssim 20$
$De \sim 2$	Wagging	~ 40
$De \gtrsim 5$	Steady-state	$\gtrsim 10^2$

The sequence of transitions with increasing Ericksen number observed earlier for small molecule nematics and reported here for polymeric nematics is summarized in the first half of table 1. Order of magnitude estimates of the shear rates, $\dot{\gamma}$, at which these transitions would be expected for an initially homeotropic $100\,\mu$ thick monodomain are reported. The shear-rate regime in which 'domain theories' are expected to apply is also indicated in table 1.

4.2. *The Deborah number cascade*

The refinement of the texture that occurs at high Ericksen number by large viscous stresses, which can exert significant torques on domains that become ever smaller as the shear rate increases. Eventually, the shear rate is high enough for individual molecules to experience significant viscous torques [43], and the molecular order parameter can be distorted from its equilibrium value. This occurs when the Deborah number, $De \equiv \lambda\dot{\gamma}$, approaches or exceeds unity [44], where λ is the average molecular relaxation time. At these high shear rates, the dynamics of polymeric nematics are dominated not by the Ericksen number, but by the Deborah number, De, and the continuum Leslie–Ericksen theory must be replaced by a molecular theory, such as that of Doi [44]. According to computations with the Doi molecular theory, as De increases, a new series of transitions in the dynamics of polymeric nematics occurs [19, 45] (see the second half of table 1); these predicted transitions have been confirmed by viscoelastic stress measurements [46, 47]. In particular, as the shear rate increases, the first normal stress difference, N_1, is predicted to undergo two changes in sign and the molecular dynamics change from 'tumbling' to 'wagging' to 'steady state'. These predicted sign changes in N_1 have been observed in viscoelastic stress measurements, the associated changes in molecular dynamics occur at the values of Deborah number $De \equiv \lambda\dot{\gamma}$ estimated in table 1.

The molecular relaxation time is, according to the molecular theory, given by $1/6\bar{D}_r$, where $\bar{D}_r$ is the rotary diffusivity of the rod-like molecules. This relaxation time is predicted to be extremely sensitive to the polymer molecular weight, a prediction confirmed in experiments with PBG solutions, which show that the shear rates at which the sign changes in N_1 occur have the expected sensitivity to molecular weight [38]. Our PBG's are polydisperse and so have more than a single molecular relaxation time. However, we can define an average relaxation time λ using the shear rate $\dot{\gamma}_{max}$ at which N_1 has its local positive maximum. For PBLG238, a weak positive local maximum in

N_1 occurs at $\dot{\gamma}_{max} = 10\,s^{-1}$ (see figure 11). According to Doi's molecular theory, for solutions with concentration not much higher than that needed to form a liquid crystalline state, $De \approx 0{\cdot}5$ at the first positive maximum [19, 38], which then gives $\lambda \approx 0{\cdot}05$ s, for PBLG238. The maximum negative value of N_1 for PBLG238 occurs at $\dot{\gamma} \approx 80$ (see figure 11); at this value of $\dot{\gamma}$, the molecular dynamics are predicted to undergo a transition [19], from 'wagging' to a 'steady state'. For PBDG298, rheological measurements in our laboratory show that N_1 has its first positive maximum at $\dot{\gamma} = 5\,s^{-1}$, and N_1 has its maximum negative value at $\dot{\gamma} = 40\,s^{-1}$. Hence for PBDG298, $\lambda \approx 0{\cdot}10$ s, twice as large as for PBLG238.

In figure 11, N_1 *versus* shear rate from Hongladarom *et al.*, are reproduced, along with their measured quantities Δn and A for 13·5 per cent PBLG238, which is one of the samples studied here. In figure 11, Δn is the birefringence determined from the wavelength dependence of the sample's optical retardance between crossed 45°–135° polarizers, and A is proportional to the peak-to-peak variation in retardance as a function of wavelength. 'A' can be interpreted as the degree to which the sample behaves as a homogeneously birefringent medium. Note from figure 11 that while Δn increases monotonically with increased $\dot{\gamma}$, A at first increases monotonically, then becomes noisy and suffers a local minimum, and then becomes less noisy, and increases again toward unity. $A = 1$ corresponds to a perfectly uniform birefringence. The measurements of Hongladarom *et al.* in figure 11 should be compared to the texture observations for sheared PBLG238 in figures 9 (*a*)–(*d*). Figures 9 (*a*)–(*d*) shows changes in colour that are consistent with the birefringence measurements reported in figure 11, i.e., Δn increases from 0·0018 to 0·0030 as $\dot{\gamma}$ increases from 0·1 to 40 s^{-1}. For the 250 μ

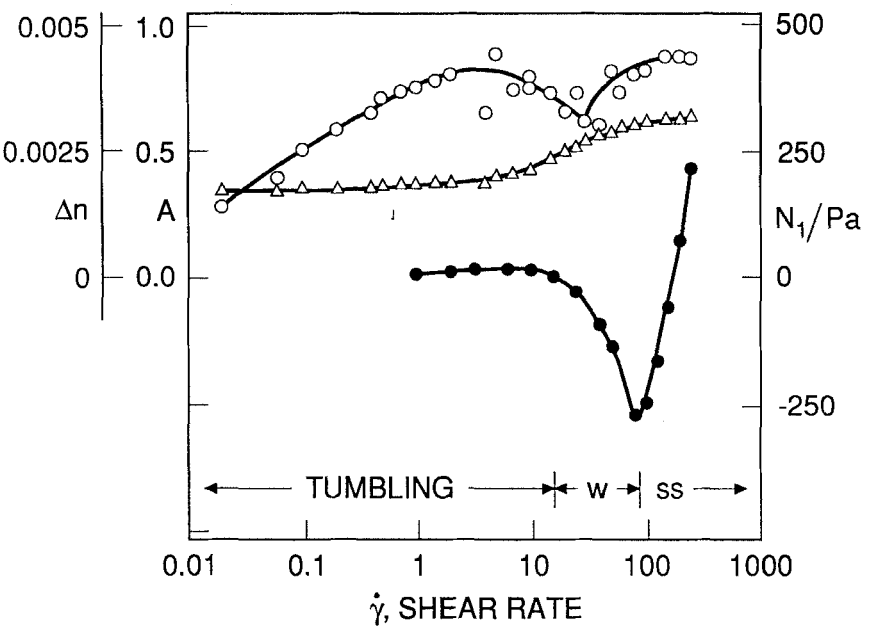

Figure 11. Amplitude, A, of retardance oscillation (○), for birefringence Δn (△), and first normal stress difference N_1 (●), for PBLG238, measured by Hongladarom *et al.* (1992), for PBLG238. Also shown are the regions of tumbling, wagging (w), and steady-state(ss) molecular dynamics, as estimated by matching the measure N_1 with that predicted from molecular theory (Larson).

thick sample we studied, this range of birefringence is equivalent to retardances ranging from 450 to 750 nm, which correspond well to the colours we observed. Also, the mottled, splotch, texture in figure 9 (*a*) is consistent with the low value of A in figure 11 for $\dot{\gamma}=0{\cdot}1\,s^{-1}$. As $\dot{\gamma}$ increases to $\dot{\gamma}=1\,s^{-1}$, the colour, shown in figure 9 (*b*), becomes more uniform, which is consistent with the increase in A reported in figure 11. Note the dip in A, beginning at $\dot{\gamma}\approx 10\,s^{-1}$, and ending at $\dot{\gamma}\approx 100\,s^{-1}$. This dip, and the associated noisiness of the data, occur over roughly the same shear rate range where we observed the distinct stripe texture, shown in figure 9 (*c*). N_1 is negative and typically quite noisy over much of this range of shear rates [48]. Finally, at $\dot{\gamma}\geqslant 75$, the texture is nearly uniform colour, which is consistent with the measured tendency, $A\rightarrow 1$ at $\dot{\gamma}\geqslant 75\,s^{-1}$ in figure 11.

These changes in birefringence and texture are no doubt linked to the changes in molecular dynamics that occur as *De* increases. At lower shear rates, around 0·1–$10\,s^{-1}$, PBLG238 is in the tumbling regime, according to the normal stress measurements. In this regime, we expect director turbulence, with the length scale of the turbulence decreasing as the shear rate increases. This is consistent with texture observations in figures 9 (*a*)–(*b*), and with the measurements in figure 11 showing A increasing with increased shear rate in this range. Since the director turbulence is expected to disrupt the average orientation of the sample, the birefringence of samples in the tumbling regime should be significantly less than that of a monodomain, which also accords with the measurements reported in figure 11.

At intermediate shear rates, around 15–$80\,s^{-1}$ for PBLG238, according to the normal stress measurements, we expect to be in the 'wagging' regime of molecular dynamics. It is in this regime of shear rates that the distinct stripes reappear for PBLG238. This regime is defined, according to the theory, by collective oscillatory motion of the molecules about an average orientation roughly in the flow direction. *A priori*, it is not obvious how the texture will respond to such molecular motions, but one would expect a degree of orientational alignment intermediate between that of the tumbling and the steady-state regimes, and this is observed both in the birefringence studies reported in figure 11, and in the colour of our micrographs in figures 9 (*c*)–(*d*). There is rheological evidence that at shear rates near the theoretically predicted transition from tumbling to wagging, the flow is susceptible to large scale flow instabilities [48] and the existence of both the dip in A in figure 11, and the relatively wide stripes in the texture shown in figure 9 (*c*), suggest that anomalous flow behaviour may occur in the wagging regime. For PBDG298, we observed distinct stripes for shear rates in the range $\dot{\gamma}=2$–$30\,s^{-1}$, which, again according to the normal stress measurements, corresponds to the wagging regime for this sample.

The easiest texture to interpret is the shear-induced monodomain that occurs at high shear rates. Theoretical calculations using the Doi theory, supported by normal stress measurements, suggest that at high shear rates, the molecules should tend toward uniform steady-state alignment in the flow direction. This steady-state alignment begins to occur, according to the theory, at a shear rate corresponding to the most negative value of N_1, which for PBLG238 is $\dot{\gamma}\approx 80\,s^{-1}$, and for PBDG298 is $\approx 40\,s^{-1}$. These shear rates are consistent with those required to obtain shear-induced monodomains, namely $\dot{\gamma}\geqslant 75\,s^{-1}$ for PBLG238, and $\dot{\gamma}\geqslant 40^{-1}$ for PBDG298. We note that these monodomains usually persist after cessation of shearing, and usually do not develop the banded texture that occurs following somewhat lower rates of shear. According to calculations using the Doi molecular theory, at shear rates in the tumbling and wagging regimes, the average molecular orientation is considerably less

than that of an ideal monodomain at rest, and this prediction accords with experimental findings, as discussed above. However, as the shear rate becomes much higher, and enters the steady-state regime, the average orientation increases, and should approach that of a monodomain. As this occurs, the tendency for molecular rearrangements upon cessation of flow should diminish. That is, if during flow the texture is defect free and the orientation in the sample is that of a stationary monodomain, there is no reason for rearrangements at the molecular or texture level to occur when flow is suddenly halted. Thus the sample should remain the same when shear flow stops, which is what Mather [41], and we, have observed. (We should note, however, that in some runs, bands formed after high rates of shearing, we believe because the motor did not stop quite quickly enough in those particular runs.)

At lower shear rates, orientation is severely disrupted by shearing flow at the molecular and/or the texture level. As a result, when flow suddenly stops, the molecules and/or the texture must rearrange themselves to find a lower energy configuration. This rearrangement tendency creates an elastic stress that is no doubt responsible for the large recoverable strains observed for these samples when the shearing stress is suddenly removed from the moving surface and strain recovery is allowed by permitting that surface to move in response to the elastic force generated by the fluid [49]. If however, the formerly moving surface is held fixed and strain recovery is not allowed, the elastic strain must be relieved some other way. Presumably the formation of bands allows for a dissipation of this elastic energy. When the moving plate is suddenly halted, we typically observe for large gaps ($d \geqslant 100\,\mu$) that a slow bulk flow persists for some time within the sample; this flow accompanies the band formation. However, when the shear rate is high enough that bands do not form, this slow flow is also absent. These observations suggest that the forces that drive elastic strain recovery also drive band formation [52].

5. Concluding remarks

Polymeric nematic or cholesteric PBG solutions undergo an extraordinary cascade of transitions with increasing shear rates; these transitions are distributed over a span of some six or more decades or more of shear rate. Remarkably, texture-free samples exist at both extremely low shear rates such that the Ericksen number, E, is low, and at extremely high shear rates where the Deborah number, De, is high. At intermediate shear rates, where most experiments have been carried out, E is large and De is small, so that the sample is highly textured and filled with disclinations and orientational inhomogeneities. As the shear rate increases, the characteristic length scale of the texture decreases from d, the gap spacing, at $E \sim 1$, to the molecular length scale at $De \sim 1$. The Ericksen number at which $De \sim 1$, so that the texture length scale reaches molecular dimensions, depends on the gap, d, and the fluid's relaxation time λ. Thus for PBG nematic solutions, there is both a lower and an upper limit on the range of Ericksen numbers over which director turbulence exists, and we expect the upper limit to depend on both d and λ. Future work should be directed toward learning whether or not this pattern of transitions observed in PBG solutions also occurs in other liquid crystalline polymers.

We thank Mohan Srinivasarao and Pat Mather for useful discussions. We give special thanks to Wesley Burghardt for discussions and for transmitting to us the data plotted in figure 11. We gratefully acknowledge Pat Cladis for advice and help.

References

[1] LESLIE, F. M., 1979, *Adv. liquid Crystals*, **4**, 1.
[2] WAHL, J., and FISCHER, F., 1973, *Molec. Crystals liq. Crystals*, **22**, 359.
[3] WAHL, J., 1979, *Z. Naturf.* (*a*), **34**, 818.
[4] GÄHWILLER, C., 1971, *Physics Lett.* A, **36**, 311.
[5] GÄHWILLER, C., 1973, *Molec. Crystals liq. Crystals*, **20**, 301.
[6] PIERANSKI, P., and GUYON, E., 1974, *Phys. Rev Lett.*, **32**, 924.
[7] GÄHWILLER, C., 1972, *Phys. Rev. Lett.*, **28**, 1554.
[8] MANNEVILLE, P., 1981, *Mol. Crystals liq. Crystals*, **70**, 223.
[9] CLADIS, P. E., and TORZA, S., 1976, *Coll. Interf. Sci.*, **4**, 487.
[10] CLADIS, P. E., and VAN SAARLOOS, W., 1992, *Solitons in Liquid Crystals*, edited by Lui Lam and Jacques Prost (Springer).
[11] TAYLOR, G. I., 1923, *Phil. Trans. R. Soc.*, **223**, 289.
[12] CHANDRASEKHAR, S., 1961, *Hydrodynamic Stability* (Clarendon Press).
[13] BRANDSTATER, A., and SWINNEY, H. L., 1987, *Phys. Rev.* A, **35**, 2207.
[14] LATHROP, D. P., FINEBERG, J., and SWINNEY, H. L., 1992, *Phys. Rev. Lett.*, **68**, 1515.
[15] KUZUU, N., and DOI, M., 1983, *J. phys. Soc. Japan*, **52**, 3486; 1984, *Ibid.* **53**, 1031.
[16] BURGHARDT, W. R., and FULLER, G. G., 1991, *Macromolecules*, **24**, 2546.
[17] SRINIVASARAO, M., and BERRY, G. C., 1991, *J. Rheol.*, **35**, 379.
[18] MARRUCCI, M., and MAFFETTONE, P. L., 1989, *Macromolecules*, **22**, 4076.
[19] LARSON, R. G., 1990, *Macromolecules*, **23**, 3983.
[20] MAGDA, J. J., BAEK, S.-G., DEVRIES, K. L., and LARSON, R. G., 1991, *Macromolecules*, **24**, 4460.
[21] PIERANSKI, P., and GUYON, E., 1974, *Phys. Rev.* A, **9**, 404.
[22] MANNEVILLE, P., and DUBOIS-VIOLETTE, E., 1976, *J. Phys., Paris*, **37**, 285.
[23] PIERANSKI, P., GUYON, E., and PIKIN, S. A., 1976, *J. Phys., Paris*, **37**, C1, 3.
[24] GUYON, E., JANOSSY, I., PIERANSKI, P., and JONATHAN, J. M., 1977, *J. Optics, Paris*, **8**, 357.
[25] DUBOIS-VIOLETTE, E., DURAND, G., GUYON, E., MANNEVILLE, P., and PIERANSKI, P., 1978, *Solid St. Phys. suppl.*, **14**, 147.
[26] SKARP, K., CARLSSON, T., LAGERWALL, S. T., and STEBLER, B., 1981, *Molec. Crystals liq. Crystals*, **66**, 199.
[27] CARLSSON, T., 1984, *Molec. Crystals liq. Crystals*, **104**, 307.
[28] CARLSSON, T., and SKARP, K., 1986, *Liq. Crystals*, **1**, 455.
[29] ZUÑIGA, I., and LESLIE, F. M., 1989, *Liq. Crystals*, **5**, 725.
[30] DERFEL, G., 1991, *Liq. Crystals*, **10**, 647.
[31] LUSKIN, M., and PAN, T.-W., 1992, *J. non-Newt. Fluid Mech.*, **42**, 369.
[32] HAN, W. H., and REY, A. D., 1991, *Materials Research Society Fall Meeting*, paper 0·7, Boston.
[33] HAN, W. H., and REY, A. D., 1992, *Theoretical and Applied Rheology*, Vol. 2, edited by P. Moldenaers and R. Keunings (Elsevier).
[34] Assuming K_1 for HBAB has a value around 10^{-6} dyn, which is typical of small molecule nematics.
[35] LARSON, R. G., 1992, *J. Rheol.* (in the press).
[36] LARSON, R. G., and MEAD, D. W., 1992, *Liq. Crystals*, **12**, 751.
[37] LEE, S.-D., and MEYER, R. B., 1990, *Liq. Crystals*, **7**, 15.
[38] GLEESON, J. T., LARSON, R. G., KISS, G., and CLADIS, P. E., 1992, *Liq. Crystals*, **11**, 341.
[39] HONGLADAROM, K., BURGHARDT, W. R., BAEK, S. G., CEMENTWALA, S., and MAGDA, J. J., 1992, *Macromolecules* (submitted).
[40] LONBERG, F., FRADEN, S., HURD, A. J., and MEYER, R. E., 1984, *Phys. Rev. Lett.*, **52**, 1903.
[41] MATHER, P. T., 1992 (private communication).
[42] LARSON, R. G., and DOI, M., 1991, *J. Rheol.*, **35**, 539.
[43] MARRUCCI, G., 1991, *Macromolecules*, **24**, 4176.
[44] DOI, M., 1980, *Ferroelectrics*, **30**, 247.
[45] LARSON, R. G., and ÖTTINGER, H. C., 1991, *Macromolecules*, **24**, 6270.
[46] KISS, G., and PORTER, R. S., 1978, *J. Polym. Sci*, **65**, 193.
[47] MAGDA, J. J., BAEK, S.-G., DE VRIES, K. L., and LARSON, R. G., 1991, *Macromolecules*, **24**, 4460.
[48] MAGDA, J. J., BAEK, S. G., DE VRIES, K. L., and LARSON, R. G., 1991, *Polymer*, **32**, 1794.
[49] LARSON, R. G., and MEAD, D. W., 1989, *J. Rheol.*, **33**, 1251.
[50] BRUINSMA, R., and SAFINYA, C. R., 1991, *Phys. Rev.* A., **43**, 5377.
[51] SAFINYA, C. R., SIROTA, E. B., and PLANO, R. J., 1991, *Phys. Rev. Lett.*, **66**, 1986.
[52] NISHIO, Y., YAMANE, T., and TAKAHASHI, T., *J. Polym. Sci. Polym. Phys. Ed.*, **23**, 1985.